J|A|C|S ARTICLES

Published on Web 07/21/2009

A Porous Coordination Polymer Exhibiting Reversible Single-Crystal to Single-Crystal Substitution Reactions at Mn(II) Centers by Nitrile Guest Molecules

Madhab C. Das and Parimal K. Bharadwaj*

Department of Chemistry, Indian Institute of Technology Kanpur, Kanpur 208016, India

Received January 26, 2009; E-mail: pkb@iitk.ac.in

Abstract: The porous coordination polymer $\{[Mn(\mathbf{L})(H_2O)](H_2O)_{1.5}(DMF)\}_n$ (**1**) containing a water molecule coordinated at the apical position of each distorted octahedral Mn(II) center has been synthesized using the solvothermal technique by reacting $Mn(NO_3)_2 \cdot 4H_2O$ with a new flexible ligand ($\mathbf{LH_2}$) having isophthalic fragment and pyridine donors at the two ends. The coordinated water molecule could be substituted by nitrile guest molecules such as acetonitrile, acrylonitrile, allylnitrile, and crotononitrile (affording compounds **2**−**5**, respectively) without loss of crystallinity. Interestingly, compound **1** selectively captures *cis*-crotononitrile into its cavity from a mixture of cis and trans isomers. Hence, the cis isomer can be separated from the trans isomer. In each case, 1.5 lattice water molecules and a dimethylformamide (DMF) molecule are also simultaneously replaced by certain numbers of these guest molecules. When these first-generation compounds **2**−**5** are dipped in DMF at room temperature with the lid of the vial open to the atmosphere, the mother crystal **1** is regenerated in each case. Thus, all of these substitution reactions are completely reversible. Also, the first-generation compounds **2**−**5** can be interconverted among one another by dipping them in appropriate nitrile guests. All of these phenomena could be observed in single-crystal to single-crystal fashion.

Introduction

Recent years have witnessed considerable interest in porous coordination polymers (PCPs) or metal−organic frameworks (MOFs) because of their potential applications as functional materials.[1−3] One of the most important discoveries in the area of PCPs involves their flexible and dynamic properties, which are characteristic of the cooperative action of organic and inorganic moieties.[4,5] Guest-responsive changes between the solid phases are particularly intriguing. Although various cases of structural transformation (single-crystal to amorphous-phase) are known, examples of single-crystal to single-crystal (SC−SC) phase transformation[6−8] are fewer in number. Most of the reported cases involve the dimerization or polymerization of unsaturated molecules[6] or guest exchange of porous materials.[7,8] Particularly rare are reactions within the coordination spheres of transition metals. Such reactions are known in solids,[9,10] but they have often been accompanied by catastrophic failure of the crystal, thus preventing the identification of the products. As has been pointed out,[4d] many applications (e.g., catalysis and storage) do not require single-crystal transformations, but retention of single crystallinity would be essential if a crystal were to be incorporated into a device such as a substrate-triggered sensor,[4d] and could also find use in directing multiple small molecules cooperatively in chemical reactivity. Besides,

(1) (a) Kuznicki, S. M.; Bell, V. A.; Nair, S.; Hillhouse, H. W.; Jacubinas, R. M.; Braunbarth, C. M.; Toby, B. H.; Tspatsis, M. *Nature* **2001**, *412*, 720.

(2) (a) Matsuda, R.; Kitaura, R.; Kitagawa, S.; Kubota, Y.; Belosludov, R. V.; Kobayashi, T. C.; Sakamoto, H.; Chiba, T.; Takata, M.; Kawazoe, Y.; Mita, Y. *Nature* **2005**, *436*, 238. (b) Kitaura, R.; Kitagawa, S.; Kubota, Y.; Kobayashi, T.; Kindo, L.; Mita, Y.; Matsuo, A.; Kobayashi, M.; Chang, H.-C.; Ozawa, T.; Suzuki, M.; Sakata, M.; Takata, M. *Science* **2002**, *298*, 2358.

(3) (a) Chae, H. K.; Siberio-Perez, D. Y.; Kim, J. H.; Go, Y. B.; Yaghi, O. M. *Nature* **2004**, *427*, 523. (b) Yaghi, O. M.; Li, G. M.; Li, H. L. *Nature* **1995**, *378*, 703. (c) Atwood, J. L.; Barbour, L. J.; Jerga, A.; Schottel, B. L. *Science* **2002**, *298*, 1000.

(4) (a) Lee, Y. E.; Jang, S. Y.; Suh, M. P. *J. Am. Chem. Soc.* **2005**, *127*, 6374. (b) Kitagawa, S.; Uemura, K. *Chem. Soc. Rev.* **2005**, *34*, 109. (c) Bradshaw, D.; Claridge, J. B.; Cussen, E. J.; Prior, T. J.; Rosseinsky, M. J. *Acc. Chem. Res.* **2005**, *38*, 273. (d) Dobrzan'ska, L.; Lloyd, G. O.; Esterhuysen, C.; Barbour, L. J. *Angew. Chem., Int. Ed.* **2006**, *45*, 5856.

(5) (a) Uemura, K.; Kitagawa, S.; Fukui, K.; Saito, K. J. *J. Am. Chem. Soc.* **2004**, *126*, 3817. (b) Matsuda, R.; Kitaura, R.; Kitagawa, S.; Kubota, Y.; Kobayashi, T. C.; Horike, S.; Takata, M. *J. Am. Chem. Soc.* **2004**, *126*, 14063. (c) Kitaura, R.; Seki, K.; Akiyama, G.; Kitagawa, S. *Angew. Chem., Int. Ed.* **2003**, *42*, 428. (d) Seki, K. *Phys. Chem. Chem. Phys.* **2002**, *4*, 1968.

(6) (a) Gao, X.; Friscic, T.; MacGillivray, L. R. *Angew. Chem., Int. Ed.* **2004**, *43*, 232. (b) Chu, Q.; Swenson, D. C.; MacGillivray, L. R. *Angew. Chem., Int. Ed.* **2005**, *44*, 3569. (c) Papaefstathiou, G. S.; Zhong, Z.; Geng, L.; MacGillivray, L. R. *J. Am. Chem. Soc.* **2004**, *126*, 9158. (d) Nagarathinam, M.; Vittal, J. J. *Angew. Chem., Int. Ed.* **2006**, *45*, 4337.

(7) (a) Lee, E. Y.; Suh, M. P. *Angew. Chem., Int. Ed.* **2004**, *43*, 2798. (b) Su, C.-Y.; Goforth, A. M.; Smith, M. D.; Pellechia, P. J.; zur Loye, H.-C. *J. Am. Chem. Soc.* **2004**, *126*, 3576. (c) Li, H.-L.; Eddaoudi, M.; O'Keefe, M.; Yaghi, O. M. *Nature* **1999**, *402*, 276. (d) Kitagawa, S.; Kitaura, R.; Noro, S. *Angew. Chem., Int. Ed.* **2004**, *43*, 2234.

(8) (a) Biradha, K.; Hongo, Y.; Fujita, M. *Angew. Chem., Int. Ed.* **2002**, *41*, 3395. (b) Wu, C.-D.; Lin, W. *Angew. Chem., Int. Ed.* **2005**, *44*, 1958. (c) Biradha, K.; Fujita, M. *Angew. Chem., Int. Ed.* **2002**, *41*, 3392. (d) Halder, G. J.; Keppert, C. J. *J. Am. Chem. Soc.* **2005**, *127*, 7891.

(9) Alfaro, N. M.; Cotton, F. A.; Daniels, L. M.; Murillo, C. A. *Inorg. Chem.* **1992**, *31*, 2718.

(10) Hanson, K.; Calin, N.; Bugaris, D.; Scancella, M.; Sevov, S. C. *J. Am. Chem. Soc.* **2004**, *126*, 10502.

10.1021/ja9006035 CCC: $40.75 © **2009 American Chemical Society**

direct observation of the orientation the guest molecules adopt in the voids will offer ways to modify the coordination space in order to carry out chemical reactions. Our attempt here is focused on SC−SC transformations through simultaneous M−D (M = metal atom; D = ligand containing a donor atom such as O or N) bond breaking/new bond formation within PCPs. The formation of new bonds by photoinduced cross-linking reactions of organic and coordination polymers in solids is known.[6] Metal−ligand bond cleavage, exemplified by the photolytic cleavage of Mn−CO bonds within a host−guest structure, has also been reported.[11] Bond breaking and new bond formation by reversible bipy/MeOH substitution in the lattice of a Co(II) complex,[12] reversible cleavage and formation of two bonds around a Ce(III) center leading to a 3D structure from a 2D coordination polymer,[13] and a reversible exchange of apical aqua and nitrate ligands coordinated to a Co(II) center[14] observed through an SC−SC transformation by an external stimulus such as temperature have very recently been reported. It should be noted that in all three of the above cases, *intramolecular rearrangements* of the ligands take place around the metal ions in the crystal lattices. However, to our knowledge, there has been just a single report to date of SC−SC transformation through substitution reactions at a metal center by simultaneous bond breaking and bond formation by an *external* guest molecule (MeOH) in a nonporous coordination polymer.[15] Most recently, reversible loss of a weakly bound pyridine ligand from a square-pyramidal Cu(II) complex[16a] and replacement of coordinated dimethylformamide (DMF) molecules by pyridine ligands of a Zn(II) coordination polymer[16b] (though not in SC−SC fashion) have been reported. Herein, we report the crystallographic observation of a substitution reaction at a Mn(II) center by a series of external guest molecules containing a −CN group, including acetonitrile (MeCN), acrylonitrile (ACN), and allylnitrile (AN), in which the guest molecule replaces the apical aqua ligand. The uptake of a particular nitrile in the presence of others was also probed. The size selectivity of guest inclusion is exemplified by the uptake of *cis*-crotononitrile (*cis*-CTN) from a mixture of *cis*- and *trans*-CTN. A DMF molecule and 1.5 lattice water molecules are also simultaneously replaced by certain numbers of these *external* guest molecules. The metal ion is incorporated into a 3D coordination network that provides a relatively fluid cavity within the solid. Although there are reports of retention of single-crystallinity upon exchange of lattice solvent molecules,[7,8] substitution of a coordinated solvent molecule by an *external* guest molecule has scarcely been observed.[15] In this regard, the present work is the first report of SC−SC reaction in which all of the solvent molecules in a crystal lattice (both coordinated and lattice) are simultaneously replaced by *external* guest molecules. It is therefore of considerable importance to study the processes that govern cooperative fluidity in dynamic crystals with a view to gaining better insight into the fascinating phenomenon of SC transformations.

Experimental Section

Materials. 5-Aminoisophthalic acid, 4-pyridinecarboxaldehyde, metal salts, and the nitriles were acquired from Aldrich and used as received. Prior to use, solvents were purified following standard procedures.

Physical Measurements. Spectroscopic data were collected as follows: IR spectra (KBr disk, 400−4000 cm^{-1}) were recorded on a PerkinElmer Model 1320 spectrometer. X-ray powder patterns (Cu Kα radiation, 3 deg/min scan rate, 293 K) were acquired using a Siefert ISODEBYEFLEX-2002 X-ray generator or a Philips PW100 diffractometer. Thermogravimetric analysis (TGA) (5 °C/min heating rate under a nitrogen atmosphere) was performed with a Mettler Toledo Star System. ^{1}H NMR spectra were recorded on a JEOL JNM-LA500 FT instrument (500 MHz) in $CDCl_3$ with TMS as the internal standard. Microanalysis data for the compounds were obtained from CDRI, Lucknow. Adsorption isotherms were measured in a Micromeritics Tristar 3000 volumetric instrument under continuous adsorption conditions. Prior to measurement, samples were heated at 250 °C for 4 h and outgassed to 10^{-3} Torr using a Micromeritics FlowPrep degasser. The specific surface areas of the compounds were obtained by applying Brunauer−Emmett−Teller (BET) (N_2 isotherm) and Langmuir (CO_2 isotherm) analyses. The temperatures of the measurements for CO_2 and N_2 were 273 and 77 K, respectively. The *cis*- and *trans*-CTN were separated following a literature method.[17]

X-ray Structural Studies. Single-crystal X-ray data were collected at 100 K on a Bruker SMART APEX CCD diffractometer using graphite-monochromatized Mo Kα radiation (λ = 0.71069 Å). The linear absorption coefficients, scattering factors for the atoms, and anomalous dispersion corrections were taken from International Tables for X-ray Crystallography. The data integration and reduction were processed with SAINT[18] software. An empirical absorption correction was applied to the collected reflections with SADABS[19] using XPREP.[20] The structure was solved by the direct methods using SHELXTL[21] and refined on F^2 by full-matrix least-squares techniques using the SHELXL-97[22] program package. The non-hydrogen atoms were refined anisotropically (except as noted). The H atoms of the coordinated water molecule of **1** were located by difference Fourier synthesis. The H atoms of the noncoordinated water molecules in **1** and all of the water molecules of the regenerated crystals could not be found in the difference Fourier map. All of the other H atoms were placed in calculated positions using idealized geometries (riding model) and assigned fixed isotropic displacement parameters. Several DFIX commands were used to fix the bond distances of solvent molecules.

Synthesis of LH_2. Triethylamine (2.8 mL, 20 mmol) was added to a stirred mixture of 5-aminoisophthalic acid (0.90 g, 5 mmol), 4-pyridinecarboxaldehyde (0.49 mL, 5.2 mmol), and dry methanol (50 mL). After 1 h, the mixture became limpid, and an excess of $NaBH_4$ was slowly added at 4 °C. After 2 h at 4 °C, the solvent was concentrated in vacuo. The residue was dissolved in water (50 mL) and acidified with AcOH to pH 5−6. After filtration, the product was obtained as a pale-yellowish solid (1.2 g, 88%; mp 162 °C). ^{1}H NMR (DMSO-d_6): δ 4.57 (s, 2H, −CH_2−), 7.42 (s, 2H, C−C*H*), 7.64 (d, J = 8.6 Hz, 2H, N−CH−C*H*), 8.05 (s, 1H, C*H*−), 8.85 (d, J = 8.4 Hz, 2H, N−C*H*−). Anal. Calcd for

(11) Kawano, M.; Kobayashi, Y.; Ozeki, T.; Fujita, M. *J. Am. Chem. Soc.* **2006**, *128*, 6558.
(12) Bradshaw, D.; Warren, J. E.; Rosseinsky, M. J. *Science* **2007**, *315*, 977.
(13) Ghosh, S. K.; Zhang, J. P.; Kitagawa, S. *Angew. Chem., Int. Ed.* **2007**, *46*, 7965.
(14) Takaoka, K.; Kawano, M.; Tominaga, M.; Fujita, M. *Angew. Chem., Int. Ed.* **2005**, *44*, 2151.
(15) Supriya, S.; Das, S. K. *J. Am. Chem. Soc.* **2007**, *129*, 3464.
(16) (a) Lennartson, A.; Håkansson, M.; Jagner, S. *New. J. Chem.* **2007**, *31*, 344. (b) Farha, O. K.; Mulfort, K. L.; Hupp, J. T. *Inorg. Chem.* **2008**, *47*, 10223.
(17) Madsen, J. Q.; Lawesson, S. O. *Tetrahedron* **1974**, *30*, 3481.
(18) *SAINT*, version 6.02; Bruker AXS: Madison, WI, 1999.
(19) Sheldrick, G. M. *SADABS: Empirical Absorption Correction Program*; University of Göttingen: Göttingen, Germany, 1997.
(20) *XPREP*, version 5.1; Siemens Industrial Automation Inc.: Madison, WI, 1995.
(21) Sheldrick, G. M. *SHELXTL Reference Manual*, version 5.1; Bruker AXS: Madison, WI, 1997.
(22) Sheldrick, G. M. *SHELXL-97: Program for Crystal Structure Refinement*; University of Göttingen: Göttingen, Germany, 1997.

Scheme 1. Ligand $\mathbf{LH_2}$

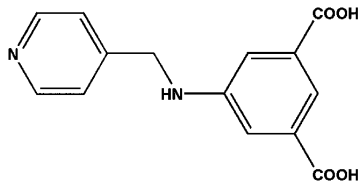

$C_{14}H_{12}N_2O_4$ (272.08): C, 61.76; H, 4.44; N, 10.29. Found: C, 61.71; H, 4.48; N, 10.33. ESI-MS (methanol) *m*/*z*: calcd for $C_{14}H_{12}N_2O_4$, 272.0797; found, 272.0805.

Synthesis of $\{[Mn(L)(H_2O)](H_2O)_{1.5}(DMF)\}_n$ (1). This compound was synthesized by mixing 1 mmol of $\mathbf{LH_2}$ and 1 mmol of $MnCl_2 \cdot 4H_2O$ in 3 mL of DMF and 1 mL of water in a Teflon-lined autoclave, which was heated under autogenous pressure to 130 °C for 36 h. Cooling to room temperature afforded the desired product as pale-pink cubic crystals in ~60% yield. The same crystalline product was obtained when the acetate or sulfate salt of Mn(II) was used in place of the chloride salt. Anal. Calcd for $C_{17}H_{23}N_3O_{7.5}Mn$: C, 45.95; H, 5.22; N, 9.46. Found: C, 45.93; H, 5.26; N, 9.50%. IR (KBr) ν (cm^{-1}): 3356, 2927, 1664, 1578, 1547, 1431, 1384.

Results and Discussion

Over the past few years, we have been exploring[23] multidentate ligands incorporating aromatic carboxylate and pyridine donors. Here we have designed the new ligand $\mathbf{LH_2}$ in which these donors are separated by a flexible spacer (Scheme 1). The compound $\{[Mn(\mathbf{L})(H_2O)](H_2O)_{1.5}(DMF)\}_n$ (**1**) was prepared using the solvothermal technique by reacting the ligand $\mathbf{LH_2}$ with $Mn(NO_3)_2 \cdot 4H_2O$ in aqueous DMF. Once formed, the crystalline product is insoluble in most organic solvents, making it possible to study the substitution reactions. Complex **1** (hereafter called the mother crystal) crystallizes in the monoclinic space group *C*2/*c*, and the asymmetric unit contains one Mn(II), one $\mathbf{L}^{2-}$, and two types of solvent molecules: one bound water molecule along with 1.5 free water molecules as well as a free DMF molecule in the channel. The Mn(II) ion is surrounded by five oxygen atoms and one nitrogen atom (Figure 1) in a distorted octahedral geometry: one water molecule and one pyridyl group occupy axial positions, and one bidentate and two bridging carboxylate groups from three different ligand moieties are at equatorial positions. The degree of distortion from the ideal octahedral geometry is reflected in the cisoid and transoid angles [58.14(9)−106.72(8) and 155.43(5)−177.4(2)°, respectively]. The Mn−N bond distance is 2.268(6) Å, and the Mn−O distances are in the range 2.099(4)−2.307(4) Å. The ligand is not planar; rather, the pyridyl group is highly twisted with respect to the phenyl ring [C−C−N−C dihedral angle = −75.71(8)°]. Two metal ions with two bridging carboxylate groups form a dimeric $\{Mn(II)\}_2$ unit with a Mn···Mn separation of 4.480(8) Å. Each of these units connects six different ligand moieties, and three such units share one ligand through one bidentate carboxylate, one chelating carboxylate, and a pyridyl N atom. These dimeric units fashion wavelike arrangements along the crystallographic *c* axis and the twisted pyridyl rings act as pillars, giving rise to an overall complicated 3D porous framework structure (Figure 2). It is worth noting that no interpenetration is observed in the structure, which possesses channels occupied by water and DMF molecules.

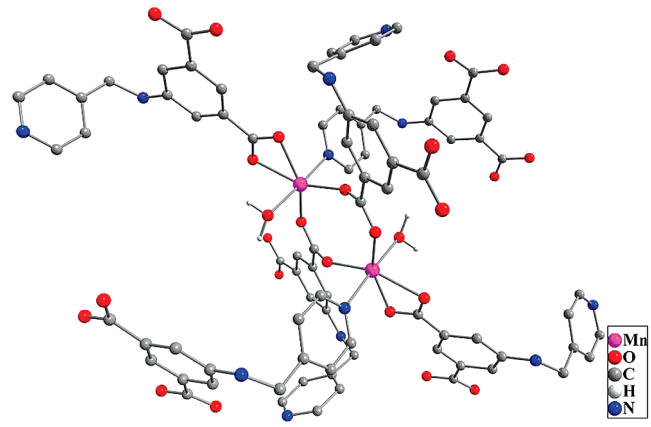

Figure 1. Dimeric unit in the crystal structure of **1** (H atoms of the ligand moieties have been omitted for clarity).

These channels are hydrophilic, since the coordinated water molecules are directed inside the channels. The channel dimensions are ~7.36 × 4.37 $Å^2$ (as measured by considering the van der Waals radii of the constituent atoms), providing a void space composed of 45.2% of the total crystal volume as estimated by PLATON.[24] C−H···O interactions among the lattice DMF molecules, O···O interactions among the coordinated and free water molecules (forming a discrete pentameric water cluster), C−H···π interactions between the C−H groups of DMF and the phenyl rings of the ligands, and intermolecular N−H···O(carboxylate) interactions (see the Supporting Information) are responsible for stabilizing the overall 3D architecture.

TGA of **1** indicates that all of the solvent molecules can be removed up to 250 °C and that no decomposition takes place up to 375 °C. It is a well-known phenomenon that guest solvent molecules located in the channels can often be removed from a framework structure without causing framework collapse, and furthermore, they can sometimes be reinserted. To explore this possibility, a single crystal of **1** was heated at 120 °C under vacuum for 2 h to yield a partially desolvated crystal, **1a**. The X-ray structure of **1a** showed that the space group had changed from *C*2/*c* to $P2_1/n$ and that the asymmetric unit consists of two Mn(II) ions, two ligand moieties, two coordinated water molecules, one lattice water molecule, and two DMF molecules. Partial expulsion of lattice water takes place, retaining the original 3D framework with the formation of two new H-bonding networks (the coordinated water molecule and the lattice water molecule together with their symmetry-related molecules form a discrete tetrameric water cluster, instead of the discrete pentameric water cluster found in **1**, the H-bonding network among the coordinated water molecules and the O atoms of the DMF molecules; see the Supporting Information). Although the coordination environment around the two metal centers remains identical to that in the mother crystal, the corresponding bond lengths and angles are slightly changed (see the Supporting Information). Most noteworthy is the increment in the length of the Mn···Mn separation by 0.166 Å in the dimeric $\{Mn(II)\}_2$ unit along with appreciable changes in the conformation of the two ligand moieties [the C−C−N−C dihedral angles are −75.02(7)° and 57.05(8)°, as opposed to −75.71(8)° found in **1**]. Because of this, the channels are much

(23) (a) Ghosh, S. K.; Savitha, G.; Bharadwaj, P. K. *Inorg. Chem.* **2004**, *43*, 5495. (b) Neogi, S.; Bharadwaj, P. K. *Inorg. Chem.* **2005**, *44*, 816.

(24) Spek, A. L. *PLATON*; The University of Utrecht: Utrecht, The Netherlands, 1999.

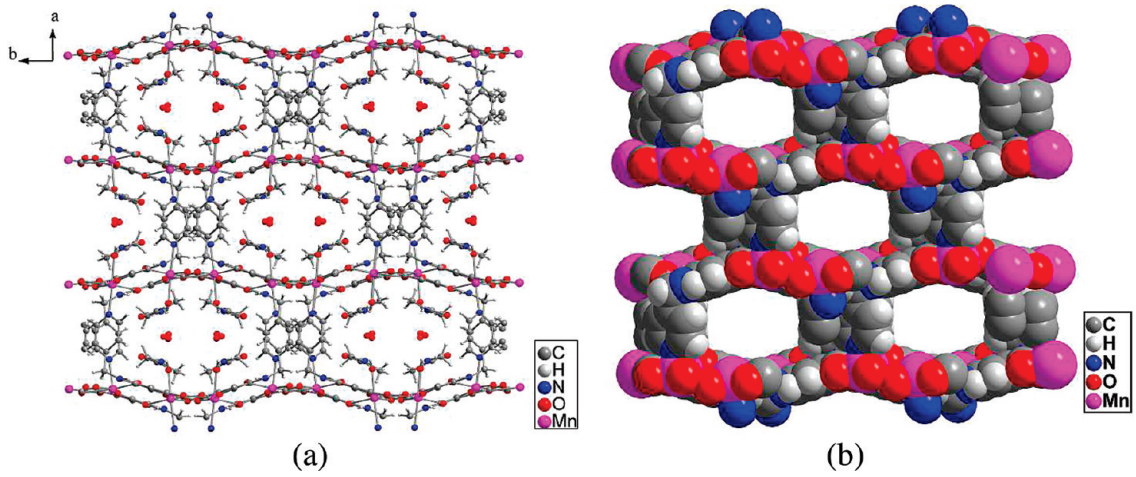

Figure 2. (a) 3D framework of **1** viewed down the crystallographic *c* axis (channels are occupied by DMF and water molecules). (b) Space-filling representation showing the pores in complex **1** (all of the solvent molecules have been omitted).

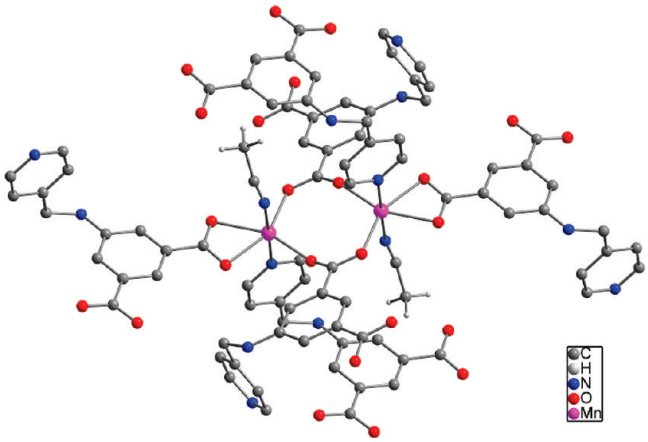

Figure 3. X-ray structure of the MeCN-substituted crystal **2** (H atoms of the ligand moieties have been omitted for clarity).

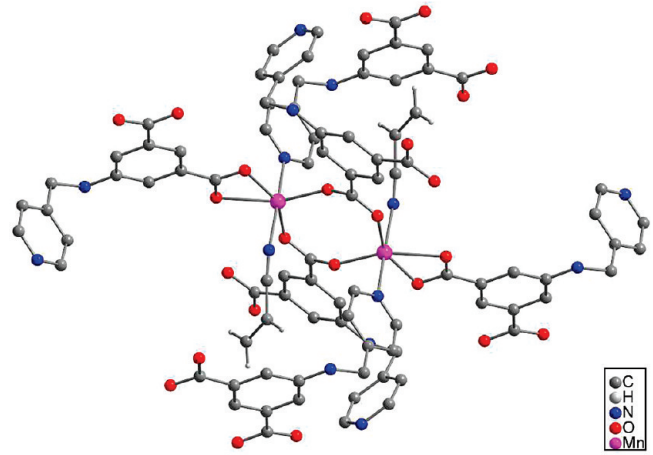

Figure 4. View of the ACN-substituted crystal **3** (for clarity, only the H atoms of the ACN molecules have been shown).

more rectangular in shape than previously. The partial loss of lattice water molecules is accompanied by a decrease of 12.03% in the cell volume (from 4188 to 3684 Å^3) and a decrease in the volume of the channel (from 45.2 to 37.9% of the total crystal volume) as well as a noteworthy shrinkage of 3.36 Å in the cell parameter along the *a* axis and an opening of the pores along the *b* axis. Exposing a crystal of **1a** to the ambient atmosphere for a day results in complete rehydration of the original structure to afford **1b**, which includes the H-bonding network observed in the original structure **1** (see the Supporting Information). In **1b**, the channel constitutes 45.4% of the total crystal volume, which is almost the same in **1**. Thus, removal and reinsertion of the guest water molecules is completely reversible. However, complete dehydration was unsuccessful, as the crystal became opaque upon heating at high temperature.

Interestingly, the crystals of **1** show a remarkable ability to substitute the coordinated water as well as lattice solvent molecules for acetonitrile. To probe SC−SC transformation with different nitriles, a mother crystal of suitable size was chosen and used throughout at room temperature (RT). When the mother crystal was immersed in acetonitrile for 4 h, it was transformed into a crystal of $\{[Mn(\mathbf{L})(MeCN)](MeCN)_{1.5}\}_n$ (**2**) (Figure 3). The structural determination of **2** revealed that the crystal system and the space group remain the same as that of the mother crystal, but the metal-bound water and lattice solvent molecules (H_2O + DMF) of **1** are completely replaced by MeCN molecules. The TGA of **2** showed that a 24% weight loss occurs at 210 °C, corresponding to 2.5 MeCN molecules in the crystal lattice, and no decomposition was observed up to 370 °C. Various C−H···N and C−H···O interactions among the MeCN molecules and the host framework appear to impart the enhancement of thermal stability (see the Supporting Information). The IR spectrum of compound **2** remained similar overall to that of compound **1** except for the appearance of a new peak at 2255 cm^{-1}, which corresponds to the C≡N stretching vibration. A packing diagram is shown in Figure S1 in the Supporting Information.

When this crystal **2** was immersed in DMF in a sample vial open to air at RT for 8 h, **2′** was obtained; X-ray structural analysis of **2′** revealed that the original mother crystal (complex **1**) was regenerated, including the H-bonding network observed in **1** (Table S1 in the Supporting Information). Thus, this substitution reaction is completely reversible.

Similar results were obtained when the mother crystal was immersed in acrylonitrile and allylnitrile to obtain $\{[Mn(\mathbf{L})(ACN)](ACN)\}_n$ (**3**) (Figure 4) and $\{[Mn(\mathbf{L})(AN)](AN)\}_n$ (**4**) (Figure 5), respectively; the crystal system and space group remained unaltered during these substitution processes. There are several C−H···O, C−H···N, and C−H···π H-bonding interactions among the solvent molecules and the host framework (see the Supporting Information). The appearance of peaks

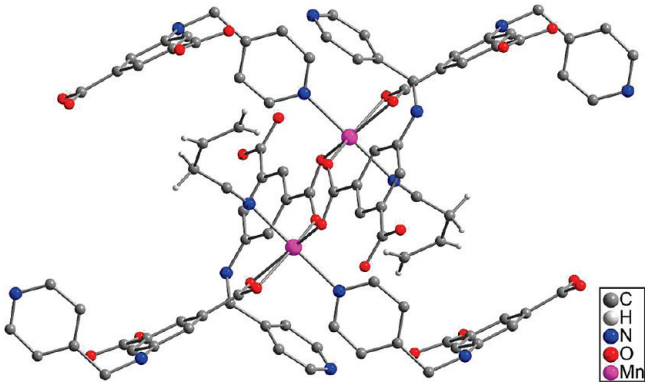

Figure 5. Representation of the AN-substituted crystal **4** (ligand H atoms have been omitted for clarity).

at 2227 and 2275 cm^{-1} in the IR spectra are attributed to the C≡N stretching vibrations for **3** and **4**, respectively. TGA of these two complexes showed that they lose all the nitrile molecules cleanly up to ∼290 °C, after which no weight loss occurs until ∼360 °C. Thus, the cavity dimensions of the mother crystal are large enough to accommodate acrylonitrile and its larger analogue, allylnitrile. The 3D array of complex **3** is displayed in Figure 6, which shows that the ACN molecules are packed in two different ways within the channels. The coordinated ones are directed toward the channel from the two wavelike walls of Mn(II) dimeric units in a face-to-face fashion with a distance of 3.541(6) Å between C17 and the centroid of the benzene moieties of alternative walls, forming C−H···π contacts. The noncoordinated ones are almost perpendicular in direction with respect to the coordinated ones within the channels (the dihedral angle between the mean planes constituted by these two types of ACN molecules is 86.66°). The point to note is that noncoordinated ACNs lie very close to the walls, with the carbon atoms (C19, C20) forming strong C−H···O contacts with two different carboxylate O atoms of a single wall. Similar interactions are observed for complex **4**: the coordinated AN molecules are in C−H···π contact, with C17 and the benzene π moieties of alternative walls at a distance of 3.449(4) Å, whereas the noncoordinated ANs are in intermolecular C−H···N interactions with the coordinated ones and also form

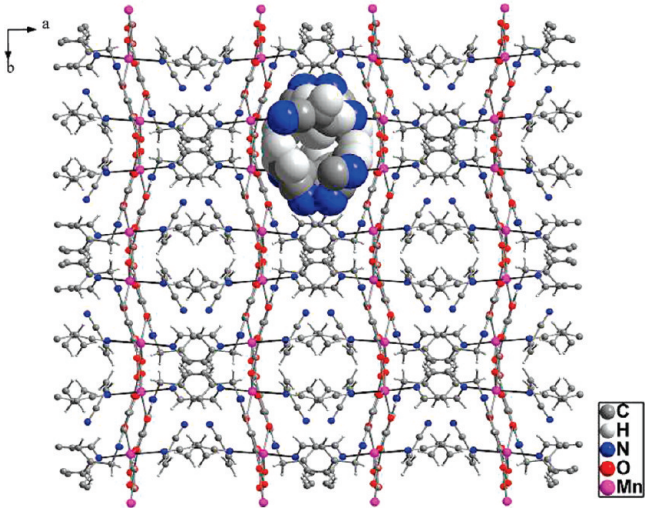

Figure 6. 3D packing diagram for **3**. The highlighted portion represents one of the channels occupied by the ACN molecules (both coordinated and noncoordinated), which are shown as a space-filling model.

Scheme 2. Nitrile Molecules Used in This Study

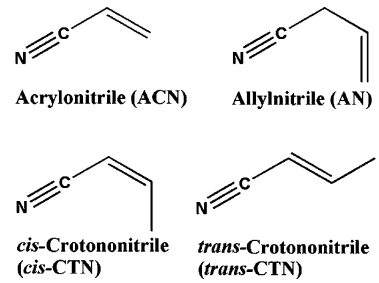

strong C−H···O contacts with the carboxylate O atoms from the nearest wall. Within the cavities, the coordinated AN molecules lie at a dihedral angle of 78.91° with respect to the noncoordinated ones. Thus, these H bonds play an important role in accommodating these nitriles in certain fashions within the channels and stabilizing the overall 3D structure with retention of single-crystallinity. A 3D packing diagram of complex **4** is depicted in Figure S2 in the Supporting Information.

Since we observed that planar ACN and AN molecules occupy special orientations within the channels, we chose to examine the reaction with crotononitrile; CTN has two geometrical isomers, with the cis isomer having an orientation very similar to ACN and AN (Scheme 2). Thus, to investigate the substitution phenomenon by CTN, the mother crystal **1** was immersed in a 40:60 (v/v) *cis*-CTN/*trans*-CTN mixture for a period of 8 h. The crystallographic determination showed that the system remains the same, yielding {[Mn(**L**)(*cis*-CTN)](*cis*-CTN)}$_n$ (**5**). Only the cis form replaces the coordinated water molecule. The other lattice solvent molecules (1.5H_2O + DMF) are also simultaneously replaced by another *cis*-CTN molecule (Figure 7). The *cis*-CTN bound to the metal is disordered, with carbon atoms C17 and C18 showing positional disorder. This was satisfactorily resolved by applying 0.75 occupancy to C17 and C18 and 0.25 occupancy to C17a and C18a. We collected the data at least five times on different single crystals, and the same results were obtained in each case. Data collected on other crystals at a slower speed indicate a structure without this disordering problem. There is a very short C−H···π interaction [3.343(6) Å] between the cis-oriented hydrogen (H17) of the coordinated *cis*-CTN and the benzene moiety, as can be seen for its above counterparts. The cis hydrogen atoms (H20 and H21) of the lattice CTN molecules are strongly H-bonded with

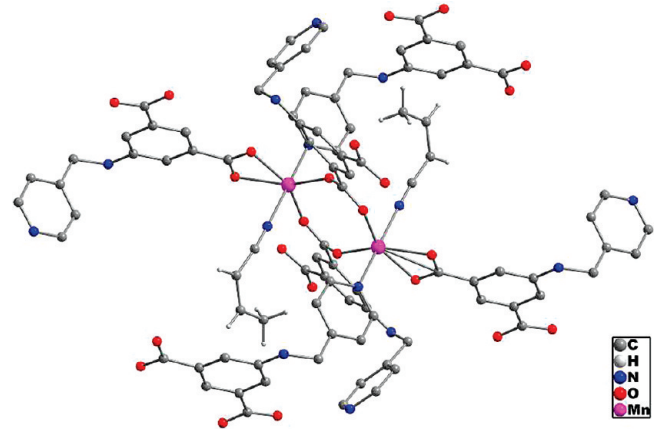

Figure 7. Dimeric unit of *cis*-CTN-substituted crystal **5** (for clarity, only the H atoms of CTN molecules have been shown).

Scheme 3. Schematic Representation of the Reversible Substitution Reactions at Mn(II) Centers within the Pores of Complex **1**

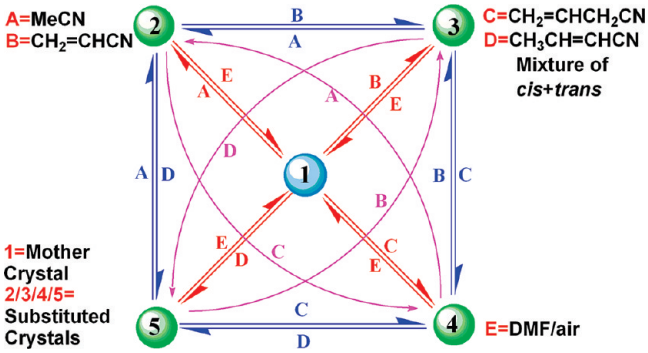

the carboxylate oxygen atoms from its nearby wall. These H-bonding interactions among the solvent molecules and the host framework sustain the porous framework structure (Table S1 in the Supporting Information). If trans isomer would have been incorporated, then possibly there would have been steric hindrance between the terminal methyl moieties and the opposite walls. To the best of our knowledge to date, there is no example of separation of geometrical isomers either by PCPs or inorganic zeolites. Such selective inclusion of geometrical isomers within the PCP is unprecedented. However, shape-selective separation of *positional isomers* of C_8 alkylaromatic compounds has been reported recently.[25] When the mother crystal **1** was immersed in pure *trans*-CTN for several days, no substitution reaction took place according to the single-crystal X-ray determination. The detailed crystallographic investigation showed that the original structure of **1**, including the H-bonding network, was preserved. In complex **5**, the dihedral angle between the planes of coordinated *cis*-CTN molecules and noncoordinated *cis*-CTN molecules is 58.3°. TGA of **5** revealed that it lost all the solvent molecules at 300 °C, with a mass loss of ∼29.4% (calculated loss of 29.2%), and no further loss occurred up to 350 °C. The band appearing at 2218 cm^{-1} in the IR spectrum is attributed to the cyanide stretching frequency of complex **5**.

To probe the selectivity further, 50, 40, 30, and 20 μL aliquots of CTN (60:40 trans/cis) were added sequentially to four sample vials containing **1** (50 mg each). After 8 h, $CDCl_3$ was added, and the liquids were transferred to NMR tubes. The gradual increase of the trans/cis ratio from 65:35 to 87:13 indicates that the cis isomer was adsorbed by complex **1**, causing the trans/cis ratio to increase (Figure S15 in the Supporting Information). The peaks corresponding to water and DMF molecules released from compound **1** were also observed in the NMR spectra.

To investigate whether these substitutions are reversible, as in the case of MeCN, the transformed crystal (**3**, **4**, or **5**) was dipped in DMF at RT with the lid of the vial open to the atmosphere. In each case, the mother crystal **1** was formed in 10−15 h (Scheme 3). The resulting crystal (**3′**, **4′**, or **5′**, respectively) showed almost the same cell dimensions as that of mother crystal **1**. In each case, the detailed crystallographic investigation showed that the original structure, including the H-bonding network, was restored (see the Supporting Information). Thus, these substitution reactions are completely reversible.

Table 1. Preference for Nitriles as Guests in **1** with Variation of Molar Ratio

MeCN/ACN/AN ratio	complex formed
1:1:0	**2**
1:0:1	**2**
1:1:1	**2**
0:1:1	**3**
1:≥5:0	**3**
1:0:≥15	**4**
0:1:≥10	**4**

In an attempt to understand the preferential substitution of one guest molecule over others, a crystal of compound **1** was immersed in mixtures of nitriles (MeCN, ACN, AN) with different proportions. When a crystal of **1** was dipped into an equimolar mixture of MeCN, ACN, and AN, only MeCN was taken up, forming a crystal of **2**. In other situations, the relative concentration of a nitrile in the mixture was found to be the deciding factor. Thus, when present in equimolar amounts in binary mixtures, MeCN is the preferred guest for **1** over either ACN or AN. Between ACN and AN, ACN is preferred. The results are collected in Table 1.

It should be noted here that none of the first-generation compounds (**2**−**5**) could be obtained by direct solvothermal synthesis. During the substitution reactions, transparency of the single-crystal was retained. The possibility of dissolution of **1** in the successive liquids followed by crystallization or renucleation at the surface and growth of the new phase was excluded by photographs of the mother crystal and its transformations to **2**, **3**, **4**, and **5** (Figure 8), which show no change in size, morphology, color, or transparency. In addition, insolubility in different nitriles was checked by NMR spectra measured with commercially available deuterated CH_3CN and $CH_2{=}CH{-}CN$ solvents after immersion of the crystals of the original compound for 10 h; these showed no peak corresponding to framework **1**. It is also notable that the formation of first-generation compounds is accompanied by the preservation of intermolecular N−H···O H-bonding interactions. Selected crystallographic parameters are summarized in Table 2.

Interestingly, the first-generation compounds (**2**−**5**) can be interconverted in SC−SC fashion by dipping them in appropriate solvents (Scheme 3). For example, dipping **2** in ACN affords **3**, and when this crystal of **3** is dipped in MeCN, **2** is regenerated. This type of interconversion among the first-generation compounds through SC−SC transformations is unprecedented.

It must be mentioned that no substitution reactions take place when a crystal of **1** is dipped in different ethers, thioethers, and

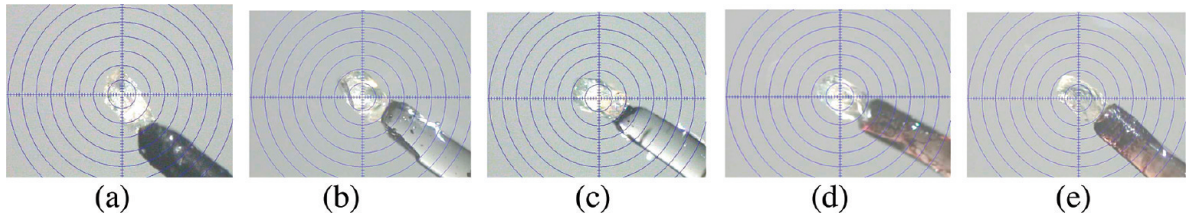

Figure 8. Photographs of single crystals of (a) **1**, (b) **2**, (c) **3**, (d) **4**, and (e) **5**.

Table 2. Crystal Data and Structure Refinement Parameters

	1	**1a**	**1b**	**2**	**3**	**4**
empirical formula	$C_{34}H_{46}Mn_2N_6O_{15}$	$C_{34}H_{40}Mn_2N_6O_{13}$	$C_{34}H_{46}Mn_2N_6O_{15}$	$C_{38}H_{35}Mn_2N_9O_8$	$C_{20}H_{16}MnN_4O_4$	$C_{22}H_{20}MnN_4O_4$
formula weight	888.65	850.60	888.65	855.63	431.31	459.36
T (K)	100(1)	100(1)	100(1)	100(1)	100(1)	100(1)
radiation	Mo Kα	Mo Kα	Mo Kα	Mo Kα	Mo Kα	Mo Kα
λ (Å)	0.71069	0.71069	0.71069	0.71069	0.71069	0.71069
cryst syst	monoclinic	monoclinic	monoclinic	monoclinic	monoclinic	monoclinic
space group	*C*2/*c*	*P*21/*n*	*C*2/*c*	*C*2/*c*	*C*2/*c*	*C*2/*c*
a (Å)	18.278(6)	14.918(5)	18.406(7)	17.777(7)	18.237(6)	18.826(7)
b (Å)	15.032(4)	15.596(5)	15.041(5)	15.303(5)	15.078(3)	14.890(2)
c (Å)	16.444(5)	16.442(5)	16.344(4)	16.267(6)	16.285(5)	16.288(4)
α (deg)	90.00	90.00	90.00	90.00	90.00	90.00
β (deg)	112.032(5)	105.606(5)	111.540(4)	113.510(5)	114.835(5)	112.937(6)
γ (deg)	90.00	90.00	90.00	90.00	90.00	90.00
V (Å^3)	4188(2)	3684(2)	4209(2)	4058(3)	4064(2)	4205(2)
Z	4	4	4	4	8	8
ρ_{calc} (Mg/m^3)	1.409	1.533	1.402	1.401	1.410	1.451
μ (mm^{-1})	0.675	0.760	0.671	0.684	0.683	0.665
F(000)	1848	1760	1848	1760	1768	1896
independent reflns	3101	4817	3122	3670	3132	2925
reflns used [$I > 2\sigma(I)$]	5204	9102	5197	4918	4968	5172
R_{int}	0.0578	0.0617	0.0573	0.0586	0.0686	0.0677
refinement method	full-matrix least-squares on F^2	full-matrix least-squares on F^2	full-matrix least-squares on F^2	full-matrix least-squares on F^2	full-matrix least-squares on F^2	full-matrix least-squares on F^2
GOF	1.065	1.044	1.053	1.051	1.075	1.047
R1, wR2 [$I > 2\sigma(I)$]	0.0615, 0.1497	0.0731, 0.1410	0.0649, 0.1511	0.0649, 0.1537	0.0720, 0.1844	0.0701, 0.1849
R1, wR2 (all data)	0.1024, 0.2141	0.1016, 0.2045	0.1011, 0.2207	0.0932, 0.2191	0.1080, 0.2440	0.1072, 0.2352
	5	**2′**	**3′**	**4′**	**5′**	
empirical formula	$C_{22}H_{20}MnN_4O_4$	$C_{34}H_{46}Mn_2N_6O_{15}$	$C_{34}H_{46}Mn_2N_6O_{15}$	$C_{34}H_{46}Mn_2N_6O_{15}$	$C_{34}H_{46}Mn_2N_6O_{15}$	
formula weight	459.36	888.65	888.65	888.65	888.65	
T (K)	100(1)	100(1)	100(1)	100(1)	100(1)	
radiation	Mo Kα	Mo Kα	Mo Kα	Mo Kα	Mo Kα	
λ (Å)	0.71069	0.71069	0.71069	0.71069	0.71069	
cryst syst	monoclinic	monoclinic	monoclinic	monoclinic	monoclinic	
space group	*C*2/*c*	*C*2/*c*	*C*2/*c*	*C*2/*c*	*C*2/*c*	
a (Å)	18.874(6)	18.409(7)	18.408(6)	18.421(5)	18.343(6)	
b (Å)	14.891(5)	15.009(6)	15.037(5)	15.029(4)	15.054(4)	
c (Å)	16.299(4)	16.341(6)	16.357(6)	16.355(5)	16.343(5)	
α (deg)	90.00	90.00	90.00	90.00	90.00	
β (deg)	114.015(2)	111.682(7)	111.575(5)	111.668(6)	111.808(4)	
γ (deg)	90.00	90.00	90.00	90.00	90.00	
V (Å^3)	4184(2)	4196(3)	4210(3)	4208(3)	4190(2)	
Z	8	4	4	4	4	
ρ_{calc} (Mg/m^3)	1.458	1.407	1.402	1.403	1.409	
μ (mm^{-1})	0.668	0.674	0.671	0.672	0.674	
F(000)	1896	1848	1848	1848	1848	
independent reflns	2675	3083	3740	3105	2970	
reflns used [$I > 2\sigma(I)$]	5233	5169	5185	5168	5155	
R_{int}	0.0710	0.0581	0.0606	0.0584	0.0556	
refinement method	full-matrix least-squares on F^2	full-matrix least-squares on F^2	full-matrix least-squares on F^2	full-matrix least-squares on F^2	full-matrix least-squares on F^2	
GOF	1.044	1.078	1.064	1.052	1.065	
R1, wR2 [$I > 2\sigma(I)$]	0.0733, 0.1870	0.0675, 0.1549	0.0645, 0.1524	0.0637, 0.1586	0.0633, 0.1515	
R1, wR2 (all data)	0.1181, 0.2406	0.1079, 0.2241	0.1064, 0.2114	0.1024, 0.2210	0.1019, 0.2186	

alcohols, or aromatic solvents such as toluene, benzene, xylene, etc. For ethers, thioethers, and alcohols, the crystal becomes opaque and does not diffract to the extent that the crystal structure can be determined. For the case of aromatic guests, the substitution reaction does not take place as well, although the crystallinity is retained, as evidened by single-crystal X-ray diffraction studies.

Sorption experiments of desolvated **1** showed that CO_2 sorption (surface area = 17.9 Å^2, kinetic diameter = 3.3 Å[26]) occurs at 273 K without any hysteresis (Figure 9), which accounts for a moderate adsorption capacity of ∼29 cm^3/g at $P/P° = 0.035$ and a specific Langmuir surface area of ∼150 m^2/g. To our surprise, no nitrogen diffusion (16.3 Å^2, 3.64 Å) was observed at 77 K (BET surface area < 1 m^2/g), despite the stable framework and adequate effective pore size. The CO_2 selectivity may be due to the higher kinetic energy of CO_2 molecules and the higher thermal energy of the coordination framework itself at 273 K, which permit diffusion of CO_2 molecules. In contrast, N_2 adsorption experiments performed at 77 K indicate that the kinetic

(25) Alaerts, L.; Kirschhock, C. E. A.; Maes, M.; van der Veen, M. A.; Finsy, V.; Depla, A.; Martens, J. A.; Baron, G. V.; Jacobs, P. A.; Denayer, J. F. M.; Vos, D. E. D. *Angew. Chem., Int. Ed.* **2007**, *46*, 4293, and references therein.

(26) Webster, C. E.; Drago, R. S.; Zerner, M. C. *J. Am. Chem. Soc.* **1998**, *120*, 5509.

(27) (a) Maji, T. K.; Matsuda, R.; Kitagawa, S. *Nat. Mater.* **2007**, *6*, 142. (b) Navarro, J. A. R.; Barea, E.; Salas, J. M.; Masciocchi, N.; Galli, S.; Sironi, A.; Ania, C. O.; Parra, J. B. *J. Mater. Chem.* **2007**, *17*, 4826.

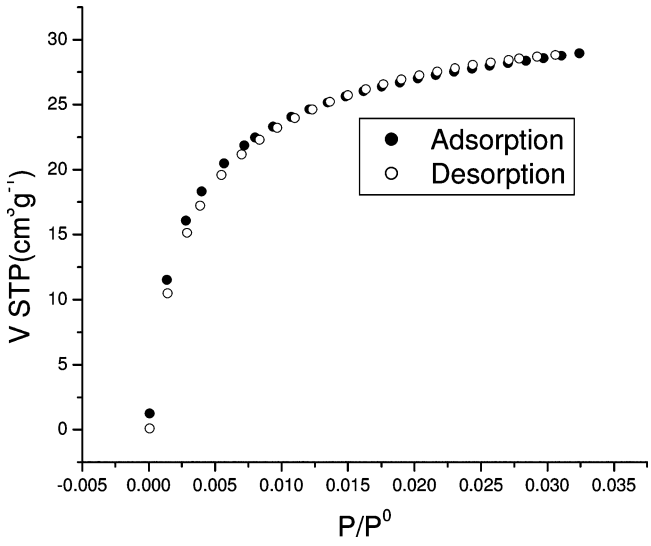

Figure 9. CO_2 adsorption isotherm of desolvated **1** at 273 K.

energy of the adsorbate and the thermal energy of the network are not high enough to permit diffusion of the adsorbate molecules through the pores.[27] Also, there is the possibility of strong interactions of N_2 with the pore window, which effectively block the pores from passing other molecules.[27a] This could also occur as a consequence of the probable partial collapse of the porous structure, as it has been found that the partial dehydration gives rise to a noteworthy shrinkage of the *a* cell parameter that along with *b* defines the opening of the pores.

Conclusion

In summary, we have succeeded in the crystallographic observation of substitution reactions of apical aqua ligands along with exchange of all other crystallized solvent molecules by a series of external nitrile guest molecules at Mn(II) centers within a 3D porous coordination network in an SC−SC fashion. Moreover, a certain shape selectivity of the porous network was observed in the selective incorporation of *cis*-CTN as opposed to *trans*-CTN. For the first time, we have observed such a selectivity in an SC−SC manner, which is unprecedented. Since ligand substitution at a metal center is a binuclear reaction, the process can only rarely be observed by X-ray crystallography. We have realized the crystallographic observation of these dynamic processes. The in situ observation of various chemical reactions in an SC−SC fashion, such as restricted cycloaddition, selective Michael Addition, etc., in the fluid cavity of these first-generation compounds is our next challenge, and the results will be reported in due course.

Acknowledgment. We gratefully acknowledge the financial support from the DST, India. M.C.D. thanks CSIR, India for SRF. We thank Prof. J. A. R. Navarro (Universidad de Granada, 18071 Granada, Spain) for gas adsorption measurements.

Supporting Information Available: Crystallographic data for **1**−**5**, **1a**, **1b**, and **2′**−**5′** (CIF); IR and TGA data; additional figures; and nonbonding distances and angles for all of the complexes. This material is available free of charge via the Internet at http://pubs.acs.org.

JA9006035